Dalton Transactions

RSC Publishing

PAPER

View Article Online
View Journal | View Issue

Assembly of trimeric polyoxovanadate aggregates based on $[MnV_{13}O_{38}]^{7-}$ building blocks and lanthanide cations†

Cite this: *Dalton Trans.*, 2013, **42**, 14445

Ding Liu,[a] Ying Lu,*[a] Yang-Guang Li,[a] Hua-Qiao Tan,[b] Wei-Lin Chen,[a] Zhi-Ming Zhang[a] and En-Bo Wang*[a]

Received 13th May 2013,
Accepted 5th August 2013

DOI: 10.1039/c3dt51250a

www.rsc.org/dalton

Three trimeric polyoxovanadate based on 1 : 13 anions $[MnV_{13}O_{38}]^{7-}$ with lanthanide cations Ln^{3+} (Ln = La, Ce and Nd) and pyridine-3-carboxylic acid: $HK_3\{[Ln(H_2O)_4]_6[MnV_{13}O_{38}]_3(SO_4)_2\}\cdot 3(C_6H_6NO_2)\cdot nH_2O$ (Ln = La **1**, Nd **3**; n = 33 for **1**, 20 for **3**), $H_{2.5}K_{1.5}\{[Ce(H_2O)_4]_6[MnV_{13}O_{38}]_3(SO_4)_2\}\cdot 3(C_6H_6NO_2)\cdot 20.5H_2O$ (**2**) ($C_6H_5NO_2$ = pyridine-3-carboxylic acid) have been synthesized and characterized by elemental analysis, IR spectroscopy, UV spectroscopy, TG analysis, XPRD, electrochemical analyses, magnetism and single-crystal X-ray diffraction. Compounds **1–3** are isostructural and crystallized in the hexagonal system, space group $P6_3/m$. Compounds **1–3** contain an unusual trimeric polyoxoanion $[\{Ln_2MnV_{13}O_{38}\}_3(SO_4)_2]^{7-}$, representing the first polyoxovanadate-based trimeric aggregate with rare earth ions. The electrochemical and electrocatalytic properties of the compounds have been investigated. Magnetic studies indicate that antiferromagnetic interactions exist in the compounds.

Introduction

Polyoxometalates (POMs), as a typical class of metal oxide clusters with nucleophilic oxygen-enriched surfaces, represent one of the excellent inorganic polydentate ligands to coordinate with transition metal or rare-earth metal ions, leading to compounds with diverse nuclearities and structural features combined with interesting catalytic, electrochemical and magnetic properties.[1] In the field of POM chemistry, the exploration of new nanoscale POM species possessing novel structures and properties is a permanent aim that researchers have been pursuing all along.[2] However, the rational design and synthesis of such compounds remain realistic and great challenges. Recently, a common strategy is using lacunary polyoxoanions as inorganic multidentate building blocks to "capture" transition metal or rare earth ions, leading to novel compounds with diverse nuclearities and structural features as well as interesting properties.[3] In this aspect, lacunary POM derivatives, such as the monovacant Dawson-type $[P_2W_{17}O_{61}]^{10-}$, trivacant Keggin-type $[PW_9O_{34}]^{9-}$ and hexavacant $[P_2W_{12}O_{48}]^{14-}$ clusters might be the candidates to incorporate more metal centers into aggregate with considerable sizes.[4] Up to now, most high-nuclear and nanoscale POM clusters are constructed by using lacunary polyoxoanions as precursor. The design and synthesis of integrity POM blocks with metal linkers should provide a promising way to achieve new types of nanoscale POM, which maintain the integrity of structure and application performance. However, the structurally integrated POM species tend to form low-dimensional (0D, 1D, or 2D) and extended three-dimensional frameworks with metal cations as linkers instead of aggregates perhaps owing to the steric demands of the POMs and the deficient charge density at their surface oxygen atoms.[5] Thus, the synthesis of high-nuclear or giant inorganic aggregates based on integrated polyoxoanions is a realistic and great challenge.

As reported in previous literature, most nanoscale POM aggregates are composed of polyoxoanion precursors containing W or Mo; the process of assembling polyoxovanadates into large oligomers or aggregates is still in its infancy,[6] perhaps due to the difference between the structural features of polyoxotungstates, polyoxomolybdates and polyoxovanadates. Therefore, the synthesis of new polyvanadate-based aggregates with novel structures and excellent properties is our pursuit. Among the various heteropolyvanadates, the unusual tridecavanadomanganate(IV) anions $[MnV_{13}O_{38}]^{7-}$ (abbreviated as $\{MnV_{13}\}$)

[a]*Key Laboratory of Polyoxometalate Science of Ministry of Education, Department of Chemistry, Northeast Normal University, Changchun, Jilin 130024, P. R. China. E-mail: luy968@nenu.edu.cn, wangeb889@nenu.edu.cn*

[b]*State Key Laboratory of Luminescence and Applications, Changchun Institute of Optics, Fine Mechanics and Physics, Chinese Academy of Sciences, 3888 East Nanhu Road, Changchun 130033, P. R. China*

†Electronic supplementary information (ESI) available: Additional structural figures, characterization, CV, XRPD, IR, UV and TG data. CCDC 937961–937963 for compounds **1–3**. For ESI and crystallographic data in CIF or other electronic format see DOI: 10.1039/c3dt51250a

seized our attention. As a polyoxovanadate, $[MnV_{13}O_{38}]^{7-}$ anion possesses higher charge density compared with polyoxomolybdate and polyoxotungstate, which makes its surface oxygen atoms have higher activity and hence they can easily bond with electrophilic linkers.[7] Furthermore, $[MnV_{13}O_{38}]^{7-}$ is a kind of functional POM, and its inhibition of tumors and bacteria activities, and catalytic oxidation performance have been extensively studied.[8] The $\{MnV_{13}\}$-based aggregates possess higher oxidation ability and further enhance the electrocatalytic sensitivity for nitrite ions, which have been a fatal threat to the environment and human health due to their toxicity and suspected carcinogenicity.

For achieving new nanoscale species based on integrated POM, we chose the reaction system of $[MnV_{13}O_{38}]^{7-}$ anion and rare earth ions (Ln^{3+}). Rare earth ions possess diverse coordination and bonding modes.[9] These features make it become more flexible in the connection with POMs and facilitate the formation of novel POM compounds with unexpected structural models and interesting properties. On the other hand, in order to obtain the aggregates based on $[MnV_{13}O_{38}]^{7-}$ anions and rare earth ions, pyridine-3-carboxylic acid molecule was selected as a protective agent. It is well known that the high reactivity of oxophilic rare earth ions with POMs always leads to precipitation instead of crystallization, which makes the elucidation of the structure difficult.[10] One of the effective methods for getting crystalline products is to adopt appropriate organic ligands during the preparation as protective agents.[11] However, the protecting method usually forms extended frameworks with POM as nodes and rare earth ions as linkers.[12] Therefore, new POM-based especially polyoxovanadate aggregates containing rare earth clusters are scarce.[13] In addition, pyridine-3-carboxylic acid may also perform the structure-directing agent role in the formation of $\{MnV_{13}\}$-based trimeric POMs, not only because it can act as the counterion in acidic solutions so as to facilitate aggregation of the polyoxoanions but also it has an appropriate volume and versatile coordination behavior, which allows extensive hydrogen bonding interactions with $[MnV_{13}O_{38}]^{7-}$ polyoxoanions.

On the basis of the aforementioned considerations, Ln cations and pyridine-3-carboxylic acid molecules were introduced into the $[MnV_{13}O_{38}]^{7-}$ system in order to explore a new route to prepare novel POM compounds with unexpected structural models and interesting properties. Herein, three unprecedented $\{MnV_{13}\}$-based trimeric polyoxovanadate aggregates, $HK_3\{[La(H_2O)_4]_6[MnV_{13}O_{38}]_3(SO_4)_2\}\cdot 3(C_6H_6NO_2)\cdot 33H_2O$ (**1**), $H_{2.5}K_{1.5}\{[Ce(H_2O)_4]_6[MnV_{13}O_{38}]_3(SO_4)_2\}\cdot 3(C_6H_6NO_2)\cdot 20.5H_2O$ (**2**) and $HK_3\{[Nd(H_2O)_4]_6[MnV_{13}O_{38}]_3(SO_4)_2\}\cdot 3(C_6H_6NO_2)\cdot 20H_2O$ (**3**), were synthesized by a conventional aqueous solution method. Compounds **1–3** contain an unusual triple-$\{MnV_{13}\}$ polyoxoanion $[\{Ln_2MnV_{13}O_{38}\}_3(SO_4)_2]^{7-}$, representing the first polyoxovanadate-based trimeric aggregate with rare earth ions in the POM chemistry. Furthermore, these polyoxoanions are well-arranged into a 3-D supramolecular assembly through hydrogen-bond interactions.

Results and discussion

Synthesis

The three nanoscale trimeric polyoxovanadates encapsulating various Ln cations were prepared by means of a carefully optimized set of experimental procedures and crystallization conditions. It can be concluded that the use of secondary organic ligands might stabilize the Ln ions and reduce the reactivity of Ln ions with polyoxoanions. Large quantities of parallel experiments indicate that pH, temperature, concentration, crystallization speed and ratio of reagents are critical synthetic parameters for the preparation of **1–3**. First, compounds **1–3** could only be obtained in the pH range 2.5–3.0. If the pH value of the reaction was lower than 2.5, only large amounts of unidentified powders were obtained. If the pH value exceeded 3.5, no crystalline products were formed as the hydrolysis of the lanthanide cation easily occurs at higher pH values. Second, the reaction temperature should remain lower than 45 °C. We have tried to increase the reaction temperature in the $[MnV_{13}O_{38}]^{7-}$/Ln systems, however, only a precipitate was obtained. Third, the filtrate must be slowly evaporate, and the crystals of title compounds were generally isolated after two weeks. If the crystallization rate was too quick it would led to crystal aggregates instead of single crystals. Moreover, the introduction of the pyridine-3-carboxylic acid molecule plays an important role in the formation of **1–3**. Attempts to replace pyridine-3-carboxylic acid with other organic molecules (pyridine-4-carboxylic acid, proline or alanine) with different sizes during the synthesis process have so far failed, suggesting that pyridine-3-carboxylic acid may act as a structure-directing agent. Trying to adopt different rare earth cations such as La^{3+}, Ce^{3+} and Nd^{3+}, we obtained the title compounds **1–3**. In addition, we have attempted to use other Ln^{3+} cations (Sm, Gd, Dy and Er) as rare earth sources; unfortunately, only a precipitate was isolated. It is presumed that the result is attributed to the lanthanide contraction effect. Similar phenomena are also observed in POM–lanthanide complexes.[14] Likewise, the contraction of the metal radius is also reflected in the decrease of the bonding Ln–O distances (Table 1). So the ionic radius of the Ln cations may play a crucial role in generating the trimers.

Structure description

Single-crystal X-ray diffraction analysis shows that compounds **1–3** are isostructural and crystallizes in the same hexagonal space group $P6_3/m$. Therefore, only the structure of compound **1** is described in detail. The basic structural unit of **1** contains

Table 1 Comparison of Ln–O bond lengths in **1–3**

Compound	Range of Ln–O lengths (Å)	Average Ln–O lengths (Å)
1 (La^{III})	2.482(6)–2.640(5)	2.570
2 (Ce^{III})	2.477(9)–2.629(8)	2.540
3 (Nd^{III})	2.444(9)–2.615(8)	2.521

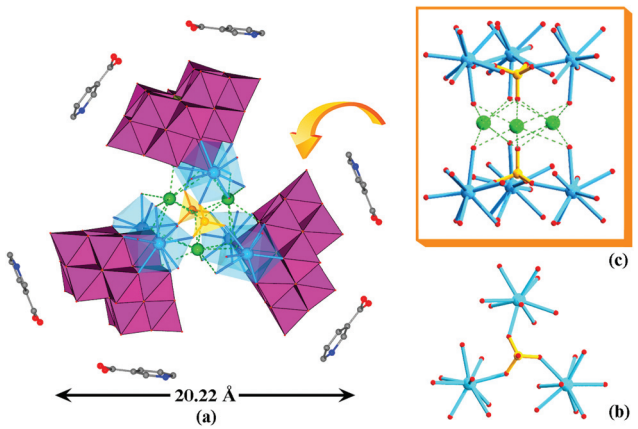

Fig. 1 Polyhedral and ball-and-stick representation of (a) the basic trimeric building blocks in **1**; (b and c) the connection modes in the rare earth cluster in **1**. Color codes: Mn (yellow), V (pink), La (blue), K (green), S (orange), C (gray), N (dark blue).

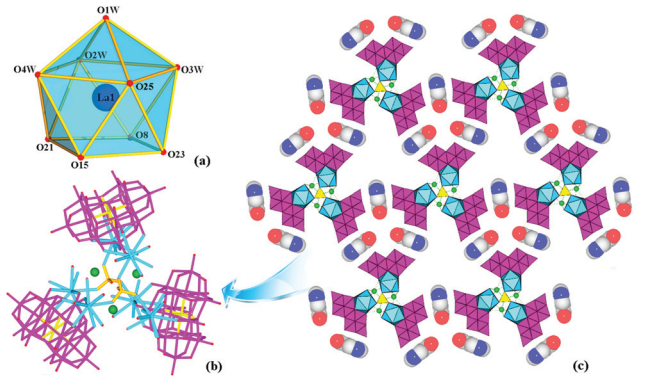

Fig. 2 (a) The coordination environments of the La^{III} cation; (b) ball-and-stick representation of the $[\{KLa_2MnV_{13}O_{38}\}_3(SO_4)_2]^{4-}$ in **1**; (c) polyhedral and space-filling representation of the 2-D supramolecular assembly of compound **1** based on POMs and pyridine-3-carboxylic acid molecules.

one triple-type POM-based shell $[La_2MnV_{13}O_{38}]_3^{3-}$ containing six trivalent lanthanide ions, two sulfate ions, three potassium ions, three protonated pyridine-3-carboxylic molecules and 33 lattice water molecules. As shown in Fig. 1a, the polyoxoanion of **1** contains three $[La_2MnV_{13}O_{38}]^{-}$ subunits, and each of them possesses an unusual 1 : 13 polyoxovanadate $[MnV_{13}O_{38}]^{7-}$. This polyoxoanion consists of thirteen edge-shared VO_6 octahedra surrounding a central Mn atom in an octahedral cavity (Fig. S1†). As revealed by X-ray crystallographic analysis, the V–O bond lengths range from 1.587 to 2.411 Å. The central Mn–O bond lengths are 1.852–1.914 Å, and the O–Mn–O angles are in the range of 87.91(6)–176.32(4)°, which are in close agreement with those described in the literature.[15] Furthermore, each $[MnV_{13}O_{38}]^{7-}$ anion is capped by two equivalent La^{3+} cations through its four terminal oxygen atoms. Simultaneously, a pair of pyridine-3-carboxylic acid molecules interact with the polyoxometalate through hydrogen bonds on the other side of the $\{MnV_{13}\}$ anion to facilitate the aggregation of polyanions (Fig. S2†). There are six La atoms which can be divided into two groups, and each set of three La ions join the central S atom to form a $\{La_3SO_4\}$ unit. In the $\{La_3SO_4\}$ subunit, each La^{3+} cation is connected with the sulfate ion in the center, and further linked to another La^{3+} cation of an adjacent $\{MnV_{13}\}$, forming the {La–O–S–O–La} bridges. The arrangement of the three La^{3+} ions around one central S atom can be regarded as an approximate trigonal-planar mode (Fig. 1b). As seen in Fig. 1c, three potassium centers are sandwiched by two parallel sets of $\{La_3SO_4\}$ units, forming a triangular prism-like structure. It is noteworthy that such high-nuclear trimeric aggregates represent the first instance of using sulfate ions as the central bridging unit in POM-based aggregate chemistry. Usually PO_4^{3-} and CO_3^{2-} were adopted as the central linker in the previous literature.[16] All of the La centers are coordinated with one O atom derived from the sulfate ligand, four terminal O atoms from the $[MnV_{13}O_{38}]^{7-}$ anion and four coordinated water molecules, exhibiting a nine-coordination environment and adopt the distorted tricapped trigonal prismatic geometry (Fig. 2a). The bond lengths of La–O are in the range of 2.482–2.640 Å. As show in Fig. 1a the external diameter of this triple-$\{MnV_{13}\}$ polyoxoanion is *ca.* 20.22 Å and the thickness is about 11.62 Å (Fig. S4†). The bond-valence sum (BVS) calculations (V 4.79, Mn 4.51, La 3.10) suggest that the V atoms are in the +5 oxidation state, the Mn atom is in the +4 oxidation state and La atoms are in the +3 oxidation state.

In the packing arrangement, compound **1** has a 3-D supramolecular structure constructed from trimeric polyoxoanions, water and pyridine-3-carboxylic acid molecules. Six protonated pyridine-3-carboxylic acid molecules act as counterions, and encapsulate the triple-$\{MnV_{13}\}$ clusters by hydrogen bonds (O···O = 2.880–3.232 Å, C···O = 2.990–3.482 Å, N···O = 3.447–3.484 Å). Synchronously, each trimeric polyoxoanion is surrounded by six adjacent polyoxoanions (Fig. 2c). On the basis of this arrangement, the polyoxoanions and the organic ligands are well-arranged into a 2-D supramolecular assembly on the *ab* plane. Furthermore, there are two kinds of such supramolecular assemblies in **1** according to the different orientations of triple-$\{MnV_{13}\}$ polyoxoanions in the layer (see Fig. 3a and b). The two kinds of layers are arranged in a staggered fashion and stacked together in an ABAB... mode along the *c* axis (Fig. 3c and d). Hence, this connection mode generates a type of hexagonal channel with an accessible size of 9.63 × 14.53 Å along the *c* axis (Fig. 4). Lattice water molecules reside in these channels and interact with polyoxoanions and pyridine-3-carboxylic acid molecules *via* hydrogen-bond interactions.

Electrochemical analyses and electrocatalytic activities

The electrochemical behaviors of compounds **1–3** and their electrocatalytic properties for nitrate were studied. The cyclic voltammetric behavior for **1** in pH 4 (0.4 M CH_3COONa–CH_3COOH) butter solution exhibits three pairs of redox peaks in the potential range of +1.4 V to −0.8 V, and the mean peak

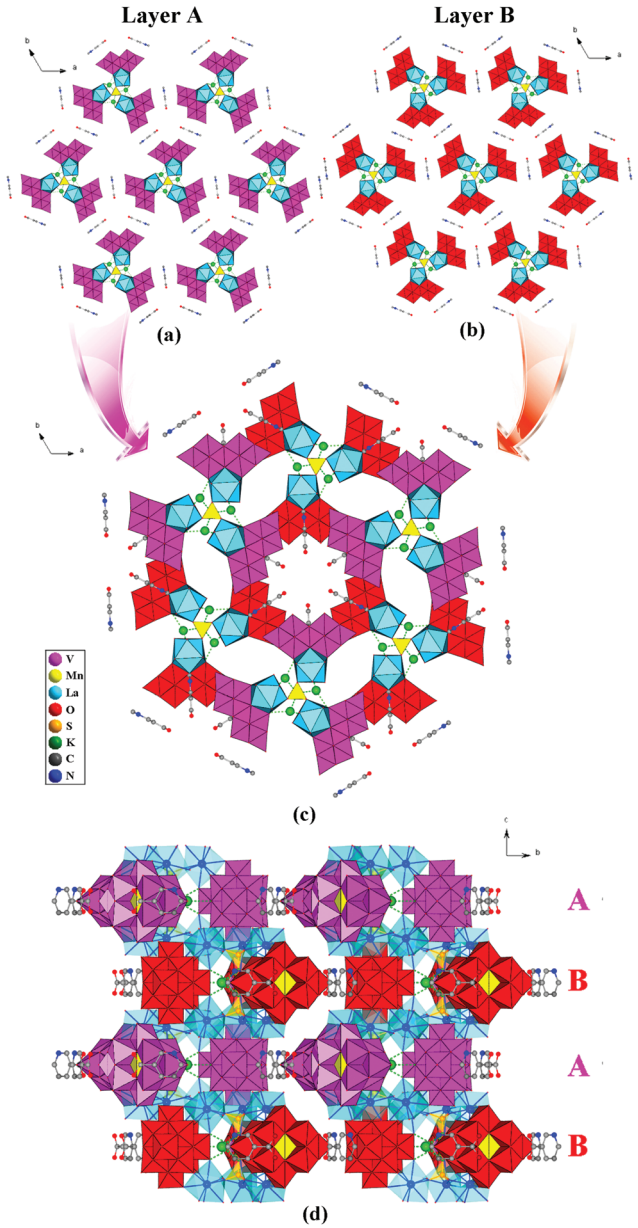

Fig. 3 (a) Layer A (pink), one 2-D supramolecular assembly of compound **1** based on trimeric {MnV_{13}}-based polyoxoanions and pyridine-3-carboxylic acid molecules; (b) layer B (red), the other 2-D supramolecular assembly of compound **1**; (c) the packing arrangement of compound **1** viewed along the *c* axis; (d) the 3-D supramolecular structure of **1** arranged in the ABAB… mode along the *a* axis.

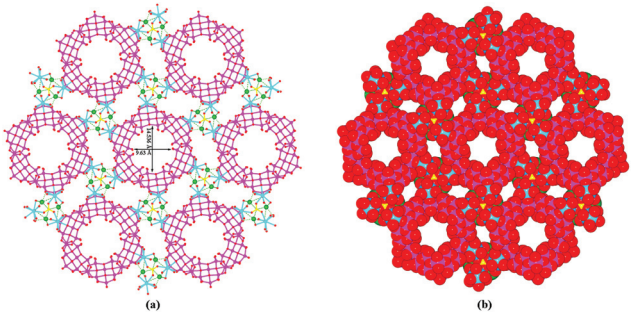

Fig. 4 (a) Ball-and-stick representation and (b) space-filling representation of the 3-D packing arrangement of **1** with channels with dimensions of 9.63 × 14.53 Å along the *c* axis. The pyridine-3-carboxylic acid and water molecules are omitted for clarity.

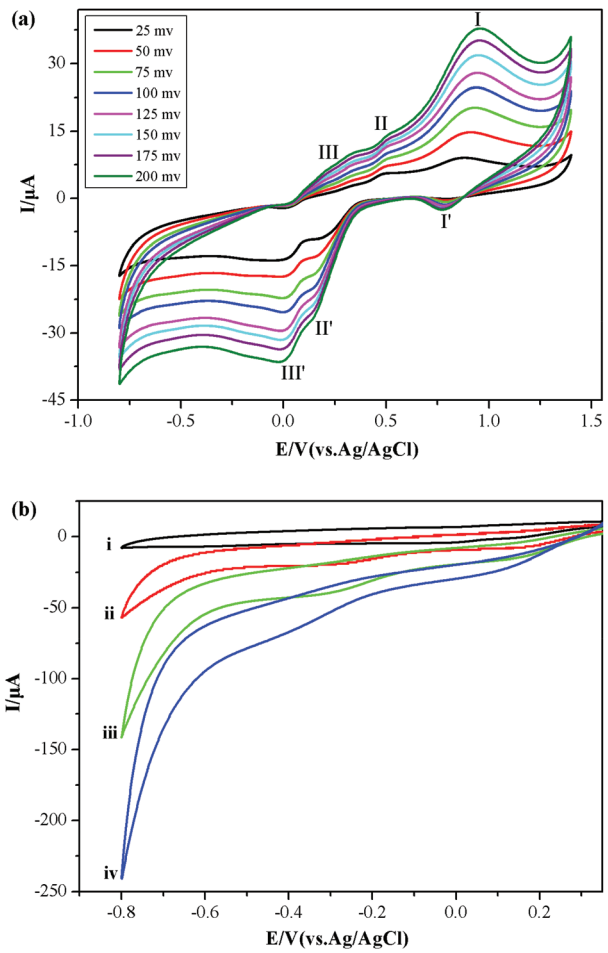

Fig. 5 (a) Cyclic voltammograms of 2 × 10^{-4} M **1** in the pH = 4.0 (0.4 M CH_3COONa + CH_3COOH) buffer solution at different scan rates (from inner to outer: 25, 50, 75, 100, 125, 150, 175, 200 mV s^{-1}); (b) electrocatalysis of the reduction of NO_2^- in the presence of 2 × 10^{-4} M **1** at the scan rate of 150 mV s^{-1}. The concentrations of NO_2^- are (i) 0.0, (ii) 1.0, (iii) 2.0, and (iv) 4.0 mM. The working electrode was glassy carbon, and the reference electrode was Ag/AgCl.

potentials, $E_{1/2} = (E_{pa} + E_{pc})/2$ are 0.861 V, 0.337 V and 0.164 V (*vs.* Ag/AgCl), respectively (Fig. 5a). The first oxidation peak I (+0.940 V) and its reduction counterpart I′ (+0.783 V) are attributed to the redox process of the Mn centers.[4c,17] The second and third oxidation peaks II and III (0.512 V and 0.321 V, respectively) and their reduction counterparts II′ and III′ (0.162 V and 0.008 V) are all ascribed to the vanadium-centered reductions, ($V^V \rightarrow V^{IV}$) and ($V^{IV} \rightarrow V^{III}$), respectively.[18]

The electrochemical properties of compound **2** were also detected in the pH 4 (0.4 M CH_3COONa + CH_3COOH) buffer solution (Fig. S7a†). There are three reduction peaks that appear in the potential range of +1.4 V to −0.8 V, with peak potentials located respectively at 0.802 V, 0.345 V and 0.109 V

versus the Ag/AgCl electrode. The oxidation peak located at 0.963 V and its reduction counterpart located at 0.642 V correspond to the redox processes of the Mn^{IV}, similar to that of **1**. The last two peaks at 0.345 V and 0.109 V are assigned to the redox process of V^{V} centers. The electrochemical properties of compound **3** were also detected in the pH 4 medium, which is similar to **1**. As shown in Fig. S8a,† there are three redox couples located in the positive domain and the mean peak potentials $E_{1/2} = (E_{pa} + E_{pc})/2$ are 0.824 V, 0.311 V and 0.151 V (*vs.* Ag/AgCl), which are ascribed to the Mn and V centers. Further, the CV of **1–3** at different scan rates showed that the peak currents of the redox process were proportional to the scan rate, indicating that the redox process on the glassy carbon (GC) electrode is surface-controlled (Fig. S9†).

The determination and elimination of nitrite ions in environmental and food samples has been paid considerable attention in recent years due to their distinct toxicity and suspected carcinogenicity.[19] Generally, it is difficult to directly electroreduce the nitrite ions to their corresponding reduced form with the bare electrode because this process requires a high overpotential at most of the bare electrode surfaces. However, the introduction of various catalysts into the bare electrodes could speed up the electroreduction process and lower the overpotential. In this aspect, POMs are one kind of suitable catalyst candidate, because POMs are capable of delivering electrons to other species, serving as powerful electron reservoirs for multielectron reductions.[20]

On the basis of the aforementioned background, the electrocatalytic reduction properties of the $\{MnV_{13}\}$-based trimeric polyoxoanions **1–3** were further investigated towards the reduction of nitrite in the same buffer solution as those employed in the CV studies. As seen in Fig. 5b, on addition of modest amounts of nitrite, the reduction peak currents of V increased, while the corresponding oxidation peak currents dramatically decreased, suggesting that nitrite was reduced by the reduced POM species. Notably, the second reduced species of **1** exhibits better electrocatalytic activity; that is, the catalytic activity is enhanced with the increasing extent of POM reduction. For **2** and **3**, the CVs for electrocatalytic reduction of nitrite were also observed under the similar conditions (Fig. S7b and S8b†). The results indicated that **1–3** display excellent electrocatalytic activity toward the reduction of nitrite. In comparison, no reduction of nitrite took place on the GC electrode in the absence of the compounds.

Magnetic properties

The variable temperature magnetic susceptibility of compound **2** was investigated in the temperature range of 2.0–300 K at a 0.1 T magnetic field on the single crystalline samples (Fig. 6). The value of χ_m increases gradually from 0.03 cm^3 mol^{-1} at 300 K to 0.20 cm^3 mol^{-1} at 41 K, then exponentially to the maximum of 2.91 cm^3 mol^{-1} at 2 K. The $\chi_m T$ *vs.* T plot decreases continuously with the decreasing temperature, and reaches 5.71 cm^3 K mol^{-1} at 2 K, revealing the characteristic of antiferromagnetic interactions. At room temperature, the experimental $\chi_m T$ value (9.89 cm^3 K mol^{-1}) of **2** is

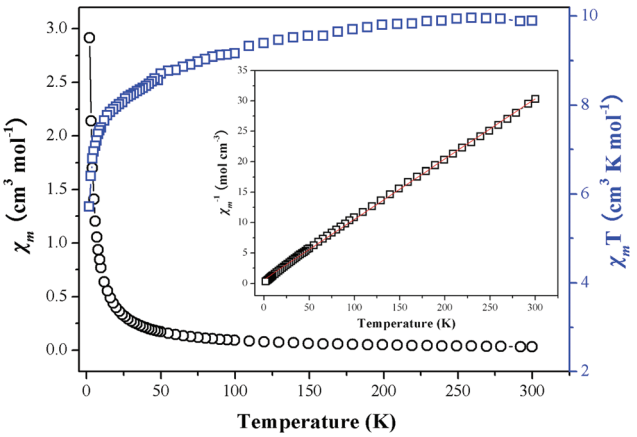

Fig. 6 The temperature dependence of χ_m (○), $\chi_m T$ (□) values and (inset) temperature dependence of reciprocal magnetic susceptibility χ_m^{-1} for **2**. The red line is the best fit with the Curie–Weiss law.

approximately equal to the theoretical value (10.44 cm^3 K mol^{-1}) for six Ce^{III} ions (4.82 cm^3 K mol^{-1}, $^2F_{5/2}$, $J = 5/2$, $g_J = 6/7$) and three isolated spin-only Mn^{IV} (5.62 cm^3 K mol^{-1}, $S = 3/2$, $g = 2.0$). As shown in Fig. 6, the magnetic susceptibility of **2** follows the Curie–Weiss law, $\chi_m = C/(T - \theta)$, with a Curie constant $C = 10.10$ cm^3 K mol^{-1} and a Weiss constant $\theta = -6.95$ K in the temperature range of 2–300 K. These Curie constants are in reasonably good agreement with the expected value. The negative Weiss temperatures suggest the presence of antiferromagnetic interactions in compound **2**. The X-ray powder diffraction pattern of the as-synthesized compound is almost identical to the calculated pattern from single-crystal diffraction data, which confirms the purity of the samples (Fig. S10†).

FT-IR and UV-Vis spectroscopy

The IR spectrum of **1** (Fig. S11†) shows a broad band at 3421 cm^{-1} and a strong peak at 1631 cm^{-1} attributed to the lattice and coordinated water molecules. The bonds at 1409 and 1109 cm^{-1} are assigned to the pyridine-3-carboxylic acid organic ligands. The characteristic peaks at 979, 927, 831, 755, 651 and 595 cm^{-1} are attributed to ν (V=O) and ν (V–O–V) in the polyoxoanions, respectively.[7] The IR spectra of **2** and **3** are similar to compound **1** (Fig. S12–S13†). The UV-vis spectra of **1–3** were recorded in aqueous solution with a concentration of 2×10^{-4} M and displayed two absorbance bonds (249 and 201 nm) in the UV region, which are attributed to the O → V charge transfer bands (Fig. S14†).[21]

TG analysis

In order to estimate the lattice-water content and thermal stability of compounds **1–3**, TG analysis was carried out from 30 to 600 °C (Fig. S15–S17†). The TG curve of compound **1** exhibits four continuous weight loss stages in the temperature ranges 38–445 °C. The first weight loss is 9.9% in the temperature range 38–114 °C, corresponding to the release of lattice water molecules in the framework (calcd 9.1%). Then, the

weight loss step of 6.4% occurred in the temperature range of 114–294 °C, mainly corresponding to the loss of the coordinated water molecules (calcd 6.6%). The following weight loss of 2.5% in the temperature range of 294–356 °C is attributed to the loss of sulfate ions (calcd 2.9%). The last weight loss of 5.2% in the temperature range of 356–445 °C could be related to the loss of pyridine-3-carboxylic acid molecules and gradual elimination of carbon deposition resulting from the complex decomposition under a N_2 atmosphere (calcd 5.7%). The whole weight loss is 24.3%, in agreement with the theoretical weight loss value (calcd 24%). In the DTA curve of **1**, the endothermic broad peak around 87.3 °C corresponds to the release of lattice and coordinated water molecules; the exothermic peak at 443 °C is attributed to the decomposition of the polyoxoanion.

Experimental section

Materials and methods

All chemicals were commercially purchased and used without further purification. $K_7[MnV_{13}O_{38}]\cdot 18H_2O$ was synthesized according to the literature and characterized by IR spectroscopy.[7a] Elemental analyses (H, N and C) were performed on a Perkin-Elmer 2400 CHN elemental analyzer; Mn, V, K, S, La, Ce and Nd were analyzed on a PLASMA-SPEC (I) ICP atomic emission spectrometer. Thermal gravimetric (TG) analyses were performed on a Perkin-Elmer TGA7 instrument in flowing N_2 with a heating rate of 10 °C min^{-1}. IR spectra were recorded in the range of 400–4000 cm^{-1} on an Alpha Centaurt FT/IR Spectrophotometer with pressed KBr pellets. UV-vis absorption spectra were obtained using a 725 PC UV-vis spectrophotometer. Powder X-ray diffraction (XRD) data were collected by using a Rigaku D/max-2550 diffractometer with Cu Kα radiation. The electrochemical measurement was carried out on a CHI 660 electrochemical workstation. All measurements were performed at room temperature. Variable-temperature magnetic susceptibility data were obtained on a SQUID magnetometer (Quantum Design, MPMS-7) in the temperature range of 2–300 K with an applied field of 0.1 T.

Synthesis of 1. $K_7[MnV_{13}O_{38}]\cdot 18H_2O$ (0.5 g, 0.26 mmol) was dissolved in 25 mL distilled water, then pyridine-3-carboxylic acid (0.08 g, 0.65 mmol) was slowly added to the orange solution, and the mixture was stirred for 30 min at 45 °C. Then, $LaCl_3$ (0.30 g, 1.2 mmol) was added to the above solution. The mixture was heated at 45 °C for 3 h after carefully adjusting the pH to 3.0 with a dilute H_2SO_4 solution (2 M). The filtrate was kept for three weeks at ambient conditions, and then yellow hexagonal-prism crystals of **1** were isolated. Yield: 50% based on $K_7[MnV_{13}O_{38}]\cdot 18H_2O$. Calcd for **1**: C, 3.32; H, 2.05; N, 0.64; K, 1.80; La, 12.78; Mn, 2.53; S, 0.98 and V, 30.48%. Found: C, 3.57; H, 1.84; N, 0.72; K, 2.13; La, 10.21; Mn, 3.08; S, 1.15 and V, 31.67%. IR (KBr pellet) for **1**: ν/cm^{-1} = 3421 (s), 1631 (m), 1409 (w), 1109 (m), 988 (s), 939 (s), 829 (m), 721 (m), 654 (s), 597 (s), 440 (m).

Synthesis of 2. The preparation of **2** was similar to that of **1** except that $Ce(NO_3)_3\cdot 6H_2O$ (0.52 g, 1.2 mmol) was used instead of $LaCl_3$. Brown crystals of **2** were harvested. Yield: 47% based on $K_7[MnV_{13}O_{38}]\cdot 18H_2O$. Calcd for **2**: C, 3.46; H, 1.77; N, 0.67; K, 0.94; Ce, 13.46; Mn, 2.64; S, 1.03 and V, 31.82%. Found: C, 3.23; H, 1.92; N, 0.75; K, 2.05; Ce, 11.76; Mn, 2.94; S, 1.17 and V, 31.52%. IR (KBr pellet) for **2**: ν/cm^{-1} = 3418 (s), 3176 (s), 1631 (s), 1385 (s), 1176 (w), 1109 (m), 986 (s), 938 (s), 828 (m), 738 (m), 654 (s), 598 (s), 440 (m).

Synthesis of 3. The preparation of **3** was similar to that of **1** except that $Nd(NO_3)_3$ (0.40 g, 1.2 mmol) was used instead of $LaCl_3$. Brown crystals of **3** were harvested. Yield: 42% based on $K_7[MnV_{13}O_{38}]\cdot 18H_2O$. Calcd for **3**: C, 3.42; H, 1.71; N, 0.66; K, 1.86; Nd, 13.70; Mn, 2.61; S, 1.01 and V, 31.45%. Found: C, 3.28; H, 1.65; N, 0.72; K, 1.69; Nd, 14.15, Mn, 2.83; S, 0.97 and V, 30.57%. IR (KBr pellet) for **3**: ν/cm^{-1} = 3742 (w), 3438 (w), 1608 (w), 1406 (m), 974 (m), 926 (m), 819 (m), 656 (s), 589 (s), 432 (s).

X-Ray crystallography

The crystallographic data were collected on a Rigaku R-axis Rapid IP diffractometer using graphite monochromatic Mo Kα radiation (λ = 0.71073 Å) and IP techniques. The crystal structures of **1–3** were solved by direct methods and refined by a full-matrix least-squares method on F^2 using the *SHELXL-97* crystallographic software package.[22] Anisotropic thermal parameters were used to refine all of the non-H atoms on the polyoxoanion and rare earth cationic cluster. During the refinement, the command 'omit -3 50' was used to omit the weak reflections above 50 degrees. In the structures of **1–3**, the C1, C2 and C5 atoms of the isolated organic molecule reside on the mirror plane and the C4 and N1 centers exhibit site-occupancy disorder with 50% for each. All the organic molecules were restrained with the command 'DFIX' so as to get a chemically reasonable structural feature. Moreover, all the organic molecule atoms were restrained with the commands 'simu' and 'isor' so as to avoid the ADP problems. Furthermore, the H atoms on the ligands could not be added due to the C/N disorder problem. In the final refinement of **1**, only four positions of the isolated lattice water molecules could be well confirmed from the residual peaks. Thus, the SQUEEZE program was used to estimate the rest of the lattice water molecules in the solvent accessible voids. It is worth mentioning that there is a relatively high residual peak (4.17 e $Å^{-3}$) close to the O2 and O5 atoms of the POM with the distances of 1.90 Å in **1**, and a relatively high residual peak (3.88 e $Å^{-3}$) close to the O21 and O22 atoms of the POM with the distances of 1.90 Å in **3**. The peaks cannot be assigned as a disordered lattice water molecule or disordered K^+ cations due to the obviously unreasonable bond distances to the O atoms of POMs. It is presumed that such residual peaks are attributed to the series termination errors. Further details of crystal data and structure refinement for compound **1–3** are summarized in Table 2. The CCDC reference numbers are 937961 (**1**), 937962 (**2**) and 937963 (**3**).

Table 2 Crystal data and structure refinements for compounds **1–3**

	1	2	3
Empirical formula	$C_{18}H_{133}K_3La_6Mn_3N_3O_{185}S_2V_{39}$	$C_{18}H_{109.5}K_{1.5}Ce_6Mn_3N_3O_{172.5}S_2V_{39}$	$C_{18}H_{107}K_3Nd_6Mn_3N_3O_{172}S_2V_{39}$
M_r	6518.63	6243.56	6316.41
Temperature (K)	298(2)	293(2)	293(2)
Crystal system	Hexagonal	Hexagonal	Hexagonal
Space group	$P6_3/m$	$P6_3/m$	$P6_3/m$
a/Å	24.559(3)	24.707(4)	24.603(3)
b/Å	24.559(3)	24.707(4)	24.603(3)
c/Å	17.082(2)	17.215(3)	17.343(3)
α/°	90.00	90.00	90.00
β/°	90.00	90.00	90.00
γ/°	120.00	120.00	120.00
V/Å^3	8922.7(18)	9101(3)	9091(2)
Z	2	2	2
D_c/g cm^{-3}	2.426	2.278	2.307
F(000)	6290	5998	6066
Reflns collected/unique	45 461/5438	65 771/5525	65 554/5523
R_{int}	0.0934	0.0916	0.1043
GOF on F^2	1.066	0.988	1.047
R_1 [a] $[I > 2\sigma(I)]$	0.0502	0.0689	0.0724
wR_2 [b]	0.1304	0.1721	0.1957
Largest residuals [e Å^{-3}]	4.175/−1.039	2.251/−1.237	4.566/−1.556

[a] $R_1 = \sum||F_o| - |F_c||/\sum|F_o|$. [b] $wR_2 = \sum[w(F_o^2 - F_c^2)^2]/\sum[w(F_o^2)^2]^{1/2}$.

Conclusions

In conclusion, three new trimeric compounds based on $\{MnV_{13}\}$ clusters encapsulating various rare earth ions and pyridine-3-carboxylic acid molecules as structure-directing agents have been successfully synthesized by a conventional aqueous solution method, providing new members of nanoscale POMs. Compounds **1–3** represent the first examples of trimeric POM aggregation based on polyoxovanadate and rare earth cations, exhibiting a 3-D supramolecular assembly with channels. The trimeric aggregate display moderately good electrocatalytic activity to reduce nitrite. Magnetic study indicates that antiferromagnetic interactions exist in compound **2**. The exploration of such POMs systems might provide a model for the preparation of new nanoscale POMs containing high-nuclear metal clusters with desirable electronic, optical and magnetic properties. This continuous research is currently going on in our group.

Acknowledgements

This work was financially supported by the National Natural Science Foundation of China (no. 20901015), the National Grand Fundamental Research 973 Program of China (2010CB635114).

Notes and references

1 (*a*) M. T. Pope, *Heteropoly and Isopoly Oxometalates*, Springer, Berlin, 1983; (*b*) E. Coronado and C. J. Gomez-Garcia, *Chem. Rev.*, 1998, **98**, 27; (*c*) T. Yamase, *Chem. Rev.*, 1998, **98**, 307; (*d*) M. I. Khan, E. Yohannes and R. J. Doedens, *Angew. Chem., Int. Ed.*, 1999, **38**, 1292; (*e*) X. K. Fang, T. M. Anderson and C. L. Hill, *Angew. Chem., Int. Ed.*, 2005, **44**, 3540; (*f*) J. Zhang, Y. F. Song, L. Cronin and T. B. Liu, *J. Am. Chem. Soc.*, 2008, **130**, 14408; (*g*) J. Zhang, J. Hao, Y. G. Wei, F. P. Xiao, P. C. Yin and L. S. Wang, *J. Am. Chem. Soc.*, 2010, **132**, 14; (*h*) M. R. Antonio, M. Nyman and T. M. Anderson, *Angew. Chem., Int. Ed.*, 2009, **48**, 6136; (*i*) U. Kortz, A. Müller, J. van Slageren, J. Schnack, N. S. Dalal and M. Dressel, *Coord. Chem. Rev.*, 2009, **253**, 2315; (*j*) M. Tonigold, Y. Lu, B. Bredenkötter, B. Rieger, S. Bahnmüller, J. Hitzbleck, G. Langstein and D. Volkmer, *Angew. Chem., Int. Ed.*, 2009, **48**, 7546; (*k*) H. N. Miras, G. J. T. Cooper, D. L. Long, H. Bögge, A. Müller, C. Streb and L. Cronin, *Science*, 2009, **327**, 72; (*l*) C. P. Pradeep, D. L. Long and L. Cronin, *Dalton Trans.*, 2010, **39**, 9443; (*m*) F. P. Xiao, J. Hao, J. Zhang, C. L. Lv, P. C. Yin, L. S. Wang and Y. G. Wei, *J. Am. Chem. Soc.*, 2010, **132**, 5956; (*n*) T. B. Liu, M. L. Langston, D. Li, J. M. Pigga, C. Pichon, A. M. Todea and A. Müller, *Science*, 2011, **331**, 1590.

2 (*a*) A. Müller, F. Peters, M. T. Pope and D. Gatteschi, *Chem. Rev.*, 1998, **98**, 239; (*b*) U. Kortz and S. Matta, *Inorg. Chem.*, 2001, **40**, 815; (*c*) D. L. Long, E. Burkholder and L. Cronin, *Chem. Soc. Rev.*, 2007, **36**, 105; (*d*) W. L. Chen, Y. G. Li, Y. H. Wang, E. B. Wang and Z. M. Su, *Dalton Trans.*, 2007, 4293; (*e*) F. Hussain, R. W. Gable, M. Speldrich, P. Kogerler and C. Boskovic, *Chem. Commun.*, 2009, 328; (*f*) S. J. Li, S. M. Liu, S. X. Liu, Y. W. Liu, Q. Tang, Z. Shi, S. X. Ouyang and J. H. Ye, *J. Am. Chem. Soc.*, 2012, **134**, 19716.

3 (*a*) B. Botar, P. Kogerler and C. L. Hill, *Inorg. Chem.*, 2007, **46**, 5398; (*b*) Y. H. Ren, S. X. Liu, R. G. Cao, X. Y. Zhao, J. F. Cao and C. Y. Gao, *Inorg. Chem. Commun.*, 2008, **11**, 1320; (*c*) Q. Wu, Y. G. Li, Y. H. Wang, E. B. Wang, Z. M. Zhang and R. Clérac, *Inorg. Chem.*, 2009, **48**, 1606; (*d*) T. McGlone, C. Streb, D. L. Long and L. Cronin, *Chem.–Asian J.*, 2009, **4**, 1612; (*e*) K. Kastner, B. Puscher and C. Streb, *Chem. Commun.*, 2012, 140; (*f*) J. Gao, J. Yan, S. Beeg, D. L. Long and L. Cronin, *J. Am. Chem. Soc.*, 2013, **135**, 1796.

4 (*a*) Z. M. Zhang, S. Yao, Y. G. Li, Y. H. Wang, Y. F. Qi and E. B. Wang, *Chem. Commun.*, 2008, 1650; (*b*) H. M. Zhang, Y. G. Li, Y. Lu, R. Clérac, Z. M. Zhang, Q. Wu, X. J. Feng and E. B. Wang, *Inorg. Chem.*, 2009, **48**, 10889; (*c*) Y. W. Li, Y. G. Li, Y. H. Wang, X. J. Feng, Y. Lu and E. B. Wang, *Inorg. Chem.*, 2009, **48**, 6452; (*d*) S. Yao, Z. M. Zhang, Y. G. Li, Y. Lu, E. B. Wang and Z. M. Su, *Cryst. Growth Des.*, 2010, **10**, 135; (*e*) S. W. Zhang, D. D. Zhang, P. T. Ma, Y. F. Liang, J. P. Wang and J. Y. Niu, *CrystEngComm*, 2013, **15**, 2992.

5 (*a*) H. Zhang, L. Y. Duan, Y. Lan, E. B. Wang and C. W. Hu, *Inorg. Chem.*, 2003, **42**, 8053; (*b*) H. Y. An, E. B. Wang, D. R. Xiao, Y. G. Li, Z. M. Su and L. Xu, *Angew. Chem., Int. Ed.*, 2006, **45**, 904; (*c*) H. Q. Tan, Y. G. Li, W. L. Chen, D. Liu, Z. M. Su, Y. Lu and E. B. Wang, *Chem.–Eur. J.*, 2009, **15**, 10940.

6 (*a*) A. Müller, E. Krickemeyer, M. Penk, R. Rohlfing, A. Armatage and H. Bogge, *Angew. Chem., Int. Ed. Engl.*, 1991, **30**, 1674; (*b*) A. Müller, R. Rohlfing, E. Krickemeyer and H. Bogge, *Angew. Chem., Int. Ed. Engl.*, 1993, **32**, 909; (*c*) L. Zhang and W. Schmitt, *J. Am. Chem. Soc.*, 2011, **133**, 11240; (*d*) J. Forster, B. Rösner, R. H. Fink, L. C. Nye, I. Ivanovic-Burmazovic, K. Kastner, J. Tucher and C. Streb, *Chem. Sci.*, 2013, **4**, 418.

7 (*a*) C. M. Flynn and M. T. Pope, *J. Am. Chem. Soc.*, 1970, **92**, 85; (*b*) S. X. Liu, D. H. Li, L. H. Xie, H. Y. Cheng, X. Y. Zhao and Z. M. Su, *Inorg. Chem.*, 2006, **45**, 8036; (*c*) Q. Lan, H. Q. Tan, D. Liu and E. B. Wang, *J. Solid State Chem.*, 2013, **199**, 129.

8 (*a*) Y. Tatsuno, C. Nakamura and T. Saito, *J. Mol. Catal.*, 1987, **49**, 57; (*b*) N. Fukuda and T. Yamase, *Biol. Pharm. Bull.*, 1997, **20**, 927; (*c*) D. Liu, Y. Lu, H. Q. Tan, W. L. Chen, Z. M. Zhang, Y. G. Li and E. B. Wang, *Chem. Commun.*, 2013, **49**, 3673.

9 (*a*) P. Mialane, A. Dolbecq, L. Lisnard, A. Mallard, J. Marrot and F. Sécheresse, *Angew. Chem., Int. Ed.*, 2002, **41**, 2398; (*b*) A. Dolbecq, P. Mialane, L. Lisnard, J. Marrot and F. Sécheresse, *Chem.–Eur. J.*, 2003, **9**, 2914; (*c*) H. Y. An, Y. G. Li, D. R. Xiao, E. B. Wang and C. Y. Sun, *Cryst. Growth Des.*, 2006, **6**, 1107; (*d*) J. P. Wang, J. W. Zhao, X. Y. Duan and J. Y. Niu, *Cryst. Growth Des.*, 2006, **6**, 507; (*e*) K. Wang, D. D. Zhang, J. C. Ma, P. T. Ma, J. Y. Niu and J. P. Wang, *CrystEngComm*, 2012, **14**, 3205.

10 C. D. Wu, C. Z. Lu, H. H. Zhuang and J. S. Huang, *J. Am. Chem. Soc.*, 2002, **124**, 3836.

11 (*a*) J. Y. Niu, D. J. Guo, J. P. Wang and J. W. Zhao, *Cryst. Growth Des.*, 2004, **4**, 241; (*b*) P. Mialane, A. Dolbecq and F. Secheresse, *Chem. Commun.*, 2006, 3477.

12 (*a*) H. Y. An, D. R. Xiao, E. B. Wang, Y. G. Li, X. L. Wang and L. Xu, *Eur. J. Inorg. Chem.*, 2005 (5), 854; (*b*) H. Y. An, D. R. Xiao, E. B. Wang, C. Y. Sun, Y. G. Li and L. Xu, *J. Mol. Struct.*, 2005, **751**, 184; (*c*) J. Lü, E. H. Shen, Y. G. Li, D. R. Xiao, E. B. Wang and L. Xu, *Cryst. Growth Des.*, 2005, **5**, 65.

13 (*a*) M. Nishio, S. Inami, M. Katayama, K. Ozutsumi and Y. Hayashi, *Inorg. Chem.*, 2012, **51**, 784; (*b*) M. Nishio, S. Inami and Y. Hayashi, *Eur. J. Inorg. Chem.*, 2013 (10–11), 1876; (*c*) M. Šimuneková, D. Prodius, V. Mereacre, P. Schwendt, C. Turta, M. Bettinelli, A. Speghini, Y. H. Lan, C. E. Anson and A. K. Powell, *RSC Adv.*, 2013, **3**, 6299; (*d*) J. M. Cameron, G. N. Newton, C. Busche, D. L. Long, H. Oshio and L. Cronin, *Chem. Commun.*, 2013, **49**, 3395.

14 (*a*) H. Y. An, Z. B. Han and T. Q. Xu, *Inorg. Chem.*, 2010, **49**, 11403; (*b*) C. Qin, X. Z. Song, S. Q. Su, S. Dang, J. Feng, S. Y. Song, Z. M. Hao and H. J. Zhang, *Dalton Trans.*, 2012, **41**, 2399.

15 (*a*) K. Nagai, H. Ichida and Y. Sasaki, *Chem. Lett.*, 1986, 1267; (*b*) D. H. Li, S. X. Liu, C. Y. Sun, L. H. Xie, E. B. Wang, N. H. Hu and H. Q. Jia, *Inorg. Chem. Commun.*, 2005, **8**, 433.

16 (*a*) R. Tsunashima, D. L. Long, H. N. Miras, D. Gabb, C. P. Pradeep and L. Cronin, *Angew. Chem., Int. Ed.*, 2010, **49**, 113; (*b*) R. Khoshnavazi, E. Naseri, S. Tayamon and A. G. Moaser, *Polyhedron*, 2011, **30**, 381; (*c*) C. Lydon, M. M. Sabi, M. D. Symes, D. L. Long, M. Murrie, S. Yoshii, H. Nojiri and L. Cronin, *Chem. Commun.*, 2012, **48**, 9819; (*d*) S. Goberna-Ferron, L. Vigara, J. Soriano-Lopez and J. R. Galan-Mascaros, *Inorg. Chem.*, 2012, **51**, 11707.

17 (*a*) X. K. Fang and P. Kogerler, *Chem. Commun.*, 2008, 3396; (*b*) X. K. Fang, K. McCallum, H. D. Pratt III, T. M. Anderson, K. Dennis and M. Luban, *Dalton Trans.*, 2012, **41**, 9867.

18 (*a*) L. H. Bi, U. Kortz, M. H. Dickman, S. Nellutla, N. S. Dalal, B. Keita, L. Nadjo, M. Prinz and M. Neumann, *J. Cluster Sci.*, 2006, **17**, 143; (*b*) C. X. Li, Y. Zhang, K. P. O'Halloran, J. W. Zhang and H. Y. Ma, *J. Appl. Electrochem.*, 2008, **39**, 421.

19 (*a*) T. R. Camp, *Water and Its Impurities*, New York, 1963; (*b*) D. E. Metzler, *Biochemistry: The Chemical Reactions of Living Cells*, New York, 1977; (*c*) A. Belhouari, B. Keita, L. Nadjo and R. Contant, *New J. Chem.*, 1998, **22**, 83; (*d*) B. S. Bassil, U. Kortz, A. S. Tigan, J. M. Clemente-Juan, B. Keita, D. P. Oliveira and L. Nadjo, *Inorg. Chem.*, 2005, **44**, 9360.

20 (*a*) T. McCormac, D. Farrell and D. G. Drennan, *Electroanalysis*, 2001, **13**, 836; (*b*) S. Cheng, T. Fernandez-Otero, E. Coronado, C. J. Gomez-Garcia, E. Martinez-Ferrero and C. J. Gimenez-Saiz, *J. Phys. Chem. B*, 2002, **106**, 7585; (*c*) X. L. Wang, Z. H. Kang, E. B. Wang and C. W. Hu,

J. Electroanal. Chem., 2002, **523**, 142; (*d*) L. D. Li, W. J. Li, C. Q. Sun and L. S. Li, *Electroanalysis*, 2002, **14**, 368; (*e*) B. Keita, I. M. Mbomekalle and L. Nadjo, *Electrochem. Commun.*, 2003, **5**, 830.

21 (*a*) Y. C. Liu, Z. F. Chen, S. M. Shi, H. S. Luo, D. C. Zhong, H. L. Zou and H. Liang, *Inorg. Chem. Commun.*, 2007, **10**, 1269; (*b*) Q. Wu, X. L. Hao, X. J. Feng, Y. H. Wang, Y. G. Li, E. B. Wang, X. Q. Zhu and X. H. Pan, *Inorg. Chem. Commun.*, 2012, **22**, 137.

22 (*a*) G. M. Sheldrick, *SHELXS97, Program for Crystal Structure Refinement*, University of Göttingen, Göttingen, Germany, 1997; (*b*) G. M. Sheldrick, *SHELXS97, Program for Crystal Structure Solution*, University of Göttingen, Göttingen, Germany, 1997.